



Simulation of PMSM Operating at Different Speeds and Optimization of PI Controller Parameters

Fatih Alpaslan KAZAN^{1*} , Osman BİLGİN² 

¹Dr., Konya Technical University, Technical Sciences Vocational School, Electronic and Automation Department, Konya, Turkey

²Prof. Dr., Karamanoglu Mehmetbey University, Faculty of Engineering, Electrical Electronics Engineering Department, Karaman, Turkey

Geliş Tarihi/Received: 15.01.2020
Kabul Tarihi/Accepted: 04.02.2020

Doi: doi.org/10.31200/makuubd.673400
Araştırma Makalesi/Research Article

ABSTRACT

This study aims to contribute to design and development studies by investigating current, speed and torque responses of permanent magnet synchronous motor (PMSM) with different loads and powers without any experimental study. For this reason, firstly, PMSM was simulated using Matlab/Simulink package program. The simulation results were then tested using a 0.25 kW PMSM coded MCS06C41, a motor driver coded EVS9322-ESV004, and the Global Drive Control interface program produced by Lenze. In addition, the model was tested on another PMSM (1.1 kW) to determine the validity of the model. Since the driver used during the experiment was designed according to field-oriented vector control, the field-oriented vector control was also preferred in the simulation. The PI controller parameters in driver simulation were optimized by using the Signal Constraint Block in Simulink Response Optimization toolbox of Matlab.

Keywords: PMSM, Field-Oriented Vector Control, Simulation, PI Parameters, Optimization.

Farklı Hızlarda Çalışan PMSM'nin Simülasyonu ve PI Denetleyici Parametrelerinin Optimizasyonu

ÖZET

Bu çalışma, farklı yüklerle ve güçlere sahip kalıcı mıknatıslı senkron motorun (PMSM) herhangi bir deneysel çalışma yapmadan akım, hız ve tork tepkilerini araştırarak tasarım ve geliştirme

çalışmalarına katkıda bulunmayı amaçlamaktadır. Bu nedenle, öncelikle PMSM'nin Matlab/Simulink paket programı kullanılarak simülasyonu yapılmıştır. Ardından simülasyon sonuçları 0.25 kW'lık MCS06C41 kodlu bir PMSM, EVS9322-ESV004 kodlu motor sürücüsü ve Lenze tarafından üretilen Global Drive Control isimli arayüz programı kullanılarak test edilmiştir. Ayrıca, model başka bir PMSM (1.1 kW) üzerinde test edilerek modelin geçerliliği incelenmiştir. Deney sırasında kullanılan sürücü alan yönlendirmeli vektör kontrolüne göre tasarlandığından, simülasyonda da alan yönlendirmeli vektör kontrolü tercih edilmiştir. Sürücü simülasyonundaki PI denetleyici parametreleri, Matlab'ın Simulink Response Optimization araç kutusundaki Signal Constraint Block kullanılarak optimize edilmiştir.

Anahtar kelimeler: PMSM, Alan Yönlendirmeli Vektör Kontrol, Simülasyon, PI Parametreleri, Optimizasyon.

1. INTRODUCTION

As it is known, synchronous motors are dual-excitation machines rotating with synchronous speed depending on the frequency of power supply and the number of motor poles. The stators of these motors are supplied with alternating current, while their rotors are supplied with direct current (DC). However, the second power supply is not needed when the rotor magnetic field is produced with permanent magnet (PM) which is placed on the rotor. Already PMSMs are also produced in this way. PMSMs use electronic drivers that provide power to the appropriate windings.

There is no rotor copper loss as there is no current on the rotor. Therefore, their efficiency is higher compared to asynchronous motors. The power factor of the motor is increased by the elimination of the component of the magnetizing current of stator current (Pragasen Pillay and Krishnan, 1989). Thus, compared to other motors it is possible to design at the same power but in smaller sizes and with better performance. When compared to asynchronous motors with the same capacity, PMSM's have advantages like a fast reaction by the reason lower inertia, a high performance due to no rotor copper loses, and smaller dimensions (Pragasen Pillay and Krishnan, 1991). These are demanded specifications by robot and plane technologies that need high power/weight ratio.

Different simulation and modeling tools are used for improving and understanding transient and steady-state behaviors of electrical driving systems. There are many studies in literature related to PMSM and its control by using Matlab/Simulink software. The validity of

these studies is decided by checking the results of the simulation (Cui et al., 2019; Lu et al., 2011; Modran, 2008; Ping and Lan, 2012; Song and Peng, 2009; Xia et al., 2019; Xiao-Ling and Hong-Hua, 2009). But comparing simulation results with results acquired from experimental studies and proving simulation validity will provide to get more realistic and correct results for further research and improvement studies. Thus, in this study, a simulation that can overlap with the experimental results of the motor is aimed.

2. MATHEMATICAL MODEL OF PMSM

The mathematical model of the motor must be well known for its control. Because the control will be done according to the designed mathematical model. Therefore the mistake on the mathematical model of the motor will cause failure in the analysis process.

The modeling of PMSM includes three mathematical models. These are;

- 3 phase model expressed on stator reference plane of variables.
- 2 phase d-q model expressed on rotor reference plane of variables.
- 2 phase α - β model quoting variables into 2 phase stable plane.

Conversion of the three-phase motor model into a two-phase model reduces the complexity of dynamic equations. 2 phases d-q model is similar to separately excited DC motor and using of this model makes control easier. Thus, solution times of equations are shortened. As it is known, in the field-oriented vector control d axis current is kept at zero, produced torque is controlled by q axis current. The mathematical model of PMSM on the rotor reference plane will be submitted with details. PMSM to be modeled is a motor that has three-phase and surface mounted.

The following assumptions are made before modeling of PMSM mathematically (Krause et al., 1986; Muni et al., 1996; Pragasan Pillay and Krishnan, 1988; Pragasen Pillay and Krishnan, 1989).

- Flux produced by PM in the air gap is sinusoidal. Hence, back electromotive force, inducted in stator windings, is sinusoidal.
- The distribution of stator windings is sinusoidal.
- There is no damper winding on the rotor.
- Polar flux depends on PM is constant.
- Saturation, eddy current, and hysteresis loss are ignored.

Accordingly, equivalent circuits of PMSM may be drawn as in Figure 1.

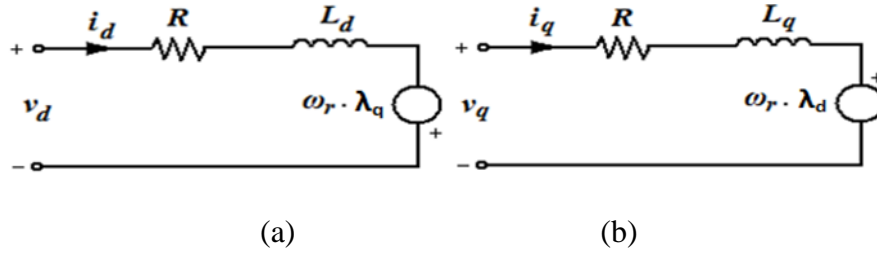


Figure 1. The equivalent circuits of PMSM (a) d axis equivalent circuit, (b) q axis equivalent circuit

By these assumptions, stator d-q voltage equations of the PMSM can be written as in Eq. (1) (Pragasan Pillay and Krishnan, 1988).

$$\begin{bmatrix} v_d \\ v_q \end{bmatrix} = \begin{bmatrix} R & 0 \\ 0 & R \end{bmatrix} \begin{bmatrix} i_d \\ i_q \end{bmatrix} + \frac{d}{dt} \begin{bmatrix} L_d & 0 \\ 0 & L_q \end{bmatrix} \begin{bmatrix} i_d \\ i_q \end{bmatrix} + \omega_r \begin{bmatrix} -\psi_q \\ \psi_d \end{bmatrix} \quad (1)$$

In Eq. (1), v_d and v_q symbolize the d-q components of the input voltage, i_d and i_q symbolize the d-q components of the phase currents, R symbolizes the resistance of the stator winding, L_d and L_q symbolize d-q axis inductances, ω_r symbolizes angular speed of the motor, finally ψ_d and ψ_q symbolize d-q axis magnetic fluxes. The d-q axis magnetic fluxes equations are given subsequently in Eq. (2).

$$\begin{bmatrix} \psi_d \\ \psi_q \end{bmatrix} = \begin{bmatrix} L_d & 0 \\ 0 & L_q \end{bmatrix} \begin{bmatrix} i_d \\ i_q \end{bmatrix} + \begin{bmatrix} \psi_m \\ 0 \end{bmatrix} \quad (2)$$

The expression of ψ_m in Eq. (2) is the magnetic flux occurred due to the PM. If Eq. (1) is written in state space form, Eq. (3) is achieved (Bilgin & Kazan, 2016).

$$\frac{d}{dt} \begin{bmatrix} i_d \\ i_q \end{bmatrix} = \left\{ \begin{bmatrix} v_d \\ v_q \end{bmatrix} - \begin{bmatrix} R & 0 \\ 0 & R \end{bmatrix} \begin{bmatrix} i_d \\ i_q \end{bmatrix} + \omega_r \begin{bmatrix} 0 & L_q \\ -L_d & 0 \end{bmatrix} \begin{bmatrix} i_d \\ i_q \end{bmatrix} - \omega_r \begin{bmatrix} 0 \\ \psi_m \end{bmatrix} \right\} \begin{bmatrix} \frac{1}{L_d} & 0 \\ 0 & \frac{1}{L_q} \end{bmatrix} \quad (3)$$

Electromagnetic torque (T_e) produced by the motor is seen at Eq. (4). The expression of p in Eq. (4) symbolizes the number of pole pairs of the motor.

$$T_e = \frac{3}{2} p \left[\lambda_m i_q + (L_d - L_q) i_q i_d \right] \quad (4)$$

When Eq. (4) is rewritten considering the equality of d-q axis inductances (Chin and Soulard, 2003; Juming et al., 2003; Modran, 2008) in surface-mounted PMSM, Eq. (5) is obtained.

$$T_e = \frac{3}{2} p \lambda_m i_q \quad (5)$$

When the Eq. (5) is examined, it will be seen that the torque to be generated by the motor can be controlled depending upon the q axis current. The angular speed (ω_r) and the position (θ_r) expressions of the rotor are seen at Eqs. (6)-(7) respectively.

$$\frac{d}{dt} \omega_r = \frac{T_e - B_m \omega_r - T_l}{J} \quad (6)$$

$$\frac{d}{dt} \theta_r = \omega_r \quad (7)$$

3. THE CONTROL OF PMSM BY USING VECTOR CONTROL METHOD

PMSMs can be controlled in three different ways. These are V/f control, directly torque control (DTC) and field effect control.

V/f control method has an advantage in middle and high-speed regions due to low cost and simple structure. Rotor position info and the high-performance processor are not needed due to an open-loop control structure. Control variables in this control method are frequency and voltage. Rate between the output frequency and the output voltage is kept constant to get a constant flux (Itoh et al., 2002).

Control variables at DTC are magnetizing flux and torque. High performance and the highest torque response are achieved at this control method in which only one PI controller is enough for speed control. The switching frequency of inverter is variable and depends on hysteresis band size and flux.

It is possible to divide field effect control into field-oriented control (FOC) and field-weakening control (FWC). The control process in both methods is done through inverting stator current into the rotating d-q axis. Q constituent of these currents is directly proportional to torque. FOC method in which d axis current is kept as zero is used especially at surface-mounted PMSM. FWC method in which the d axis current is kept at a value other than zero is widely used in internal PMSMs. FOC method has been preferred in the simulation due to the motor used in the experiment is surface mounted PMSM and the used driver is designed according to the FOC method. The block scheme of this control method is seen in Figure 2.

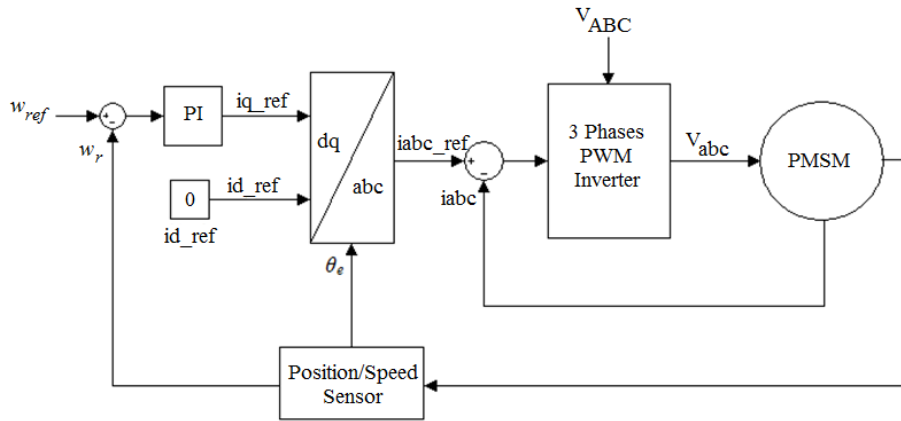


Figure 2. Principle scheme of the FOC method

4. SIMULATION OF PMSM

Simulation of PMSM was conducted by Matlab/Simulink software by using (1), (3), (4), (6), and (7) numbered equations above mentioned.

Each of the blocks created for the simulation of the motor is shown below. The blocks were formed as subsystems to enable the model to be understood and developed (Figure 3). The blocks were then combined to form the d-q axis model of the motor (Figure 4). Finally, the electromechanical speed model of the motor was created seen in Figure 5.

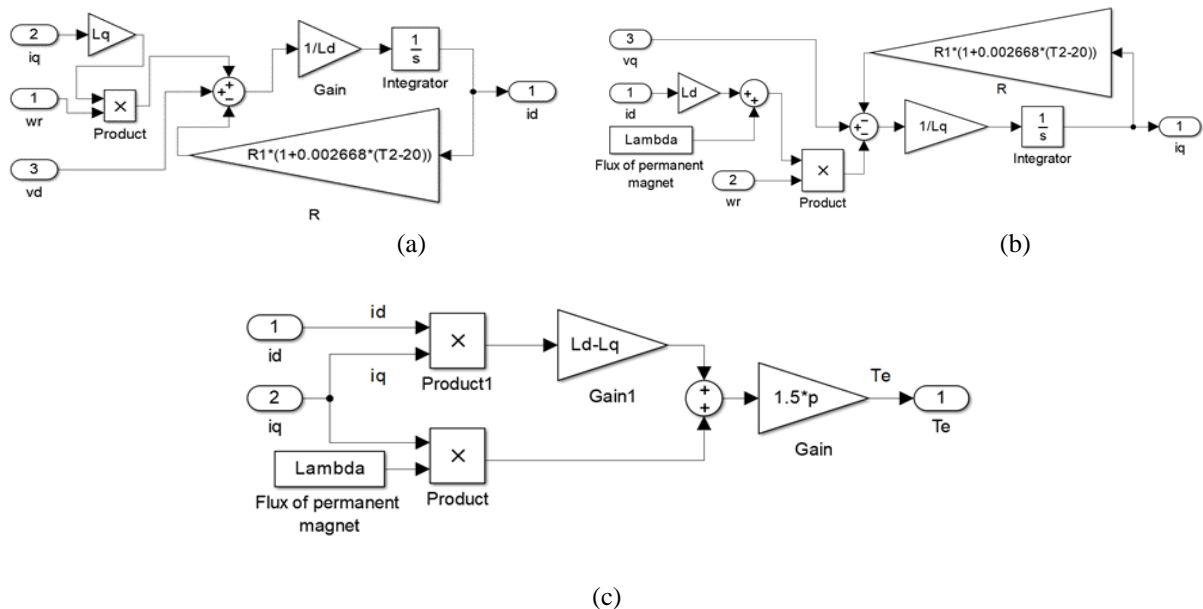


Figure 3. The internal structure of blocks which the d-q axis model (a) i_d current model, (b) i_q current model, (c) Model of the electromagnetic torque generated by the motor

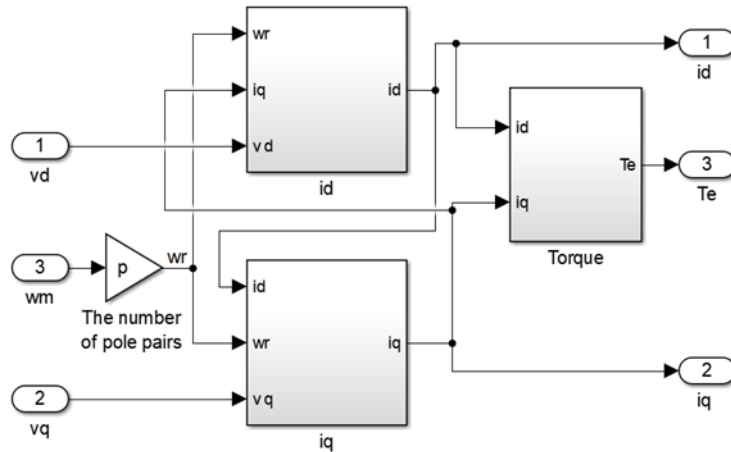


Figure 4. The d-q axis model of the PMSM

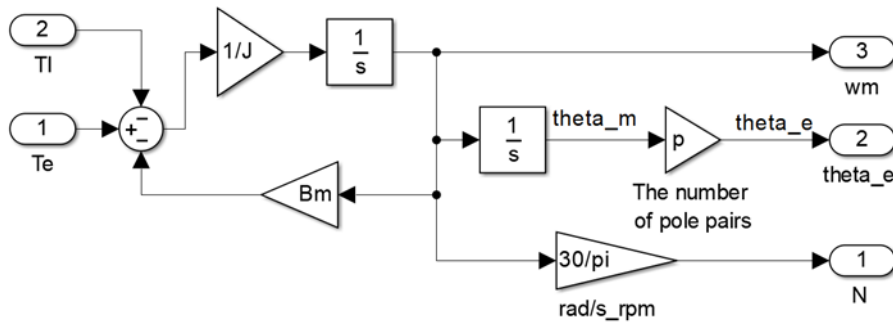


Figure 5. Electromechanical speed model of the PMSM

PWM inverter which has hysteresis current control was preferred in the simulation. In the driver simulation (Figure 6), the mechanical speed feedback was compared with the reference speed to obtain an error signal. This signal was passed through the PI controller to obtain the reference value for the current i_q . The current limiting block was used to prevent the reference current value from exceeding the maximum current value of the motor. Since the FOC method was used, the reference value for the d axis current was kept at zero. Then, the d-q current references were converted to a three-phase system with the conversion block (dq2abc) and reference current values for the three phases were obtained. These values were compared with the actual three-phase current values to generate an error signal for the three phases. It was checked whether the obtained error signals were outside the hysteresis range specified in the PWM block. If the signal was out of the hysteresis band, the polarity of the voltage applied to the respective phase winding was reversed. These processes, which were realized in a three-phase system, were transferred to the d-q plane by abc2dq block so that the motor produced the desired torque (Kazan, 2009).

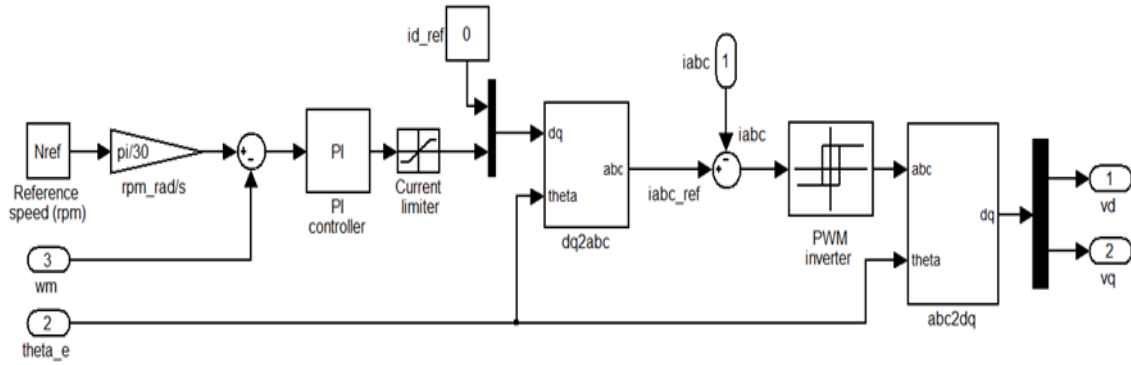


Figure 6. The simulink model of PMW driver with FOC.

PMSM's complete Simulink model with FOC is seen in Figure 7.

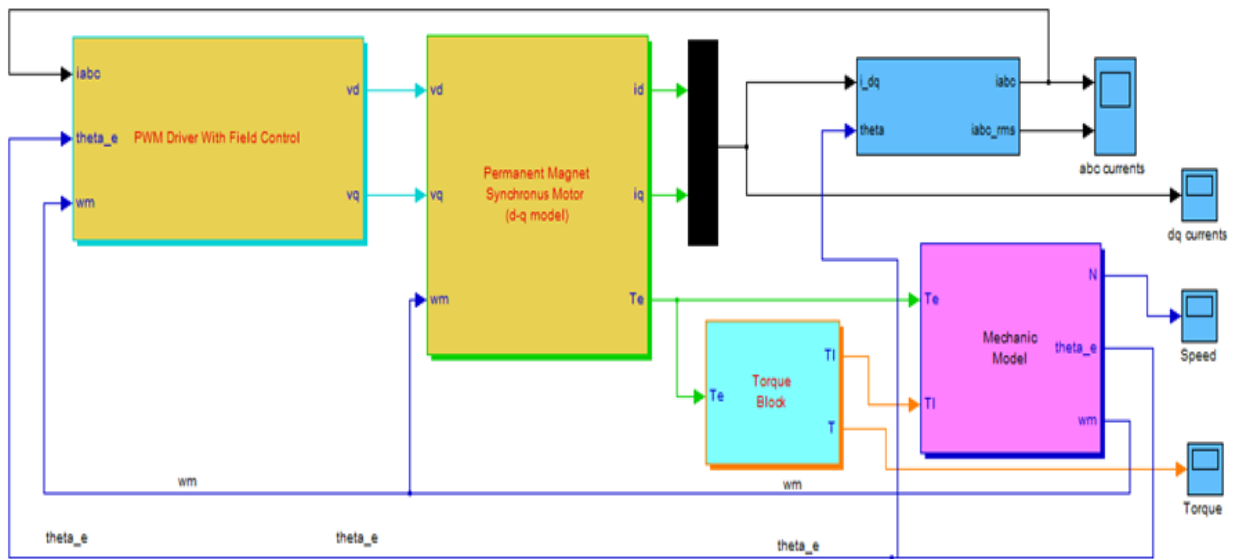


Figure 7. PMSM's complete simulink model with FOC

5. OPTIMIZATION OF PI CONTROLLER PARAMETERS

The parameters of the PI controller in the field-oriented PWM driver shown in Figure 8 were optimized by the Signal Constraint block in the Simulink Response Optimization toolbox. The optimization is done by placing this block in the relevant section where it is desired to optimize the step response of the system. Since the speed response will be optimized in the simulation, the relevant block was placed on the speed feedback as shown in Figure 8.

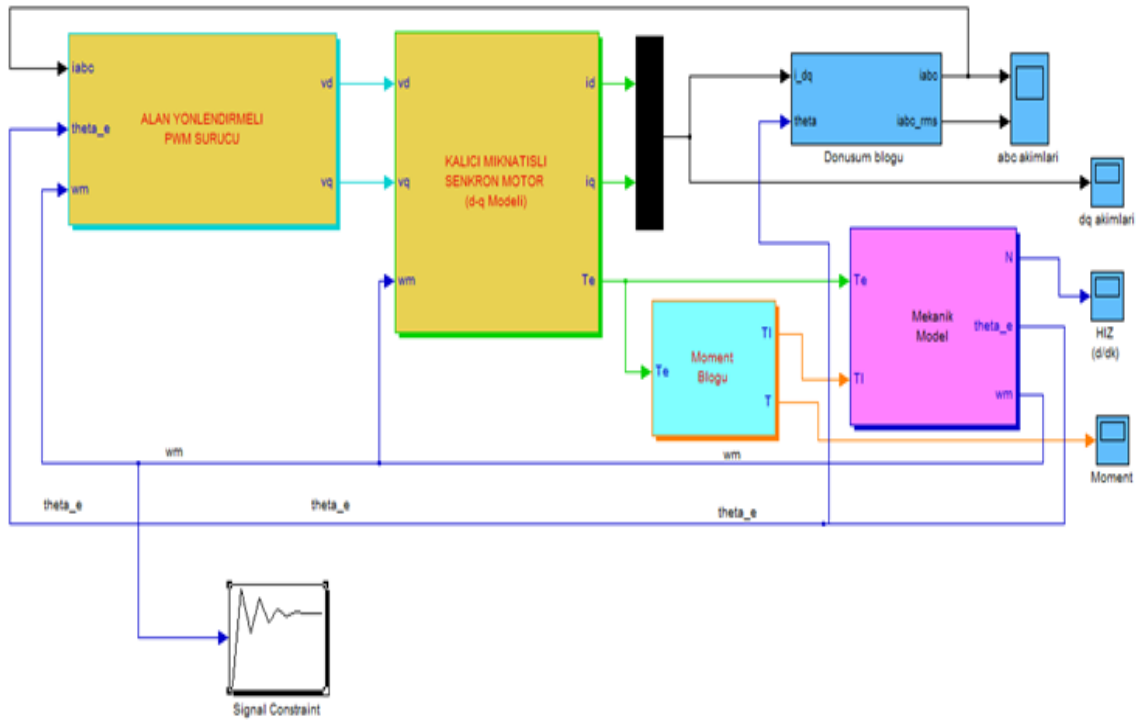


Figure 8. Inserting of the signal constraint block into the PMSM model

It is possible to determine the desired step response characteristics such as rise time, settling time and overshoot. *Desired Response* under the Goals menu in the *Signal Constraint* window is selected to determine the step response characteristics (Figure 9). Another way to achieve this is by clicking the right mouse button in an empty space in the *Signal Constraint* window and clicking *Desired Response* from the pop-up menu. When this process is done, the window shown in Figure 10 will be reached.

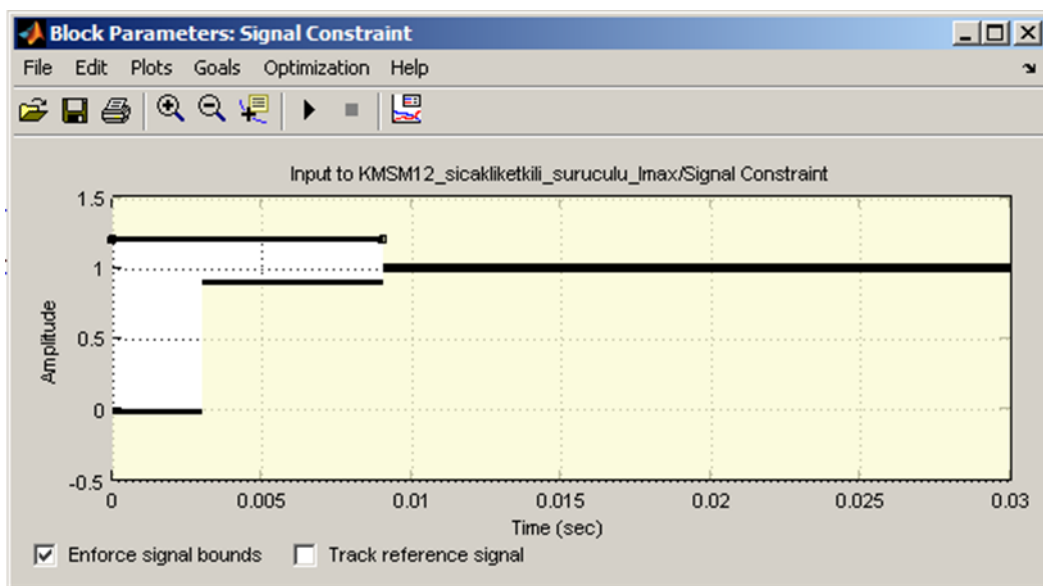


Figure 9. Signal Constraint window that the optimization process is managed

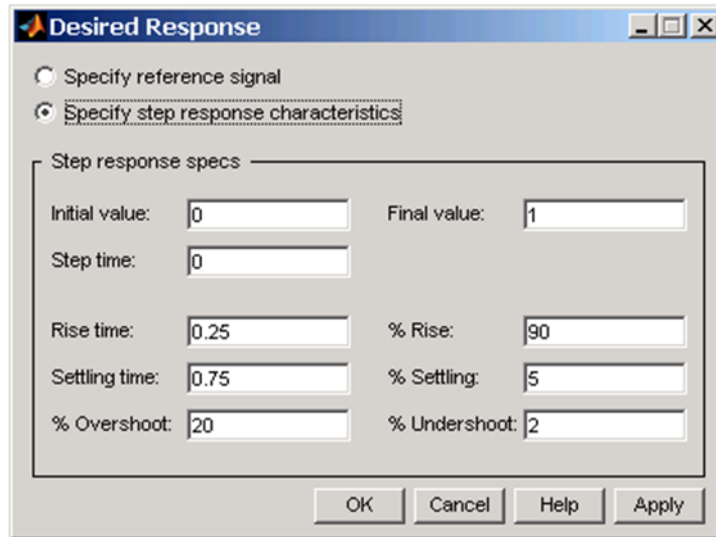


Figure 10. Desired Response window that step response characteristics are determined

In the window of Figure 10, the desired initial value, final value, step time, rise time, rise in %, settling in %, overshoot and undershoot in % are determined. Thus the limits of optimization are determined. The PI parameters (K_p and K_i) are then assigned as variables in the Matlab (workspace). These variables are assigned as variables in the optimization process using the *Tuned Parameters* option under the *Optimization* menu shown in the window in Figure 9. This screen is shown in Figure 11.

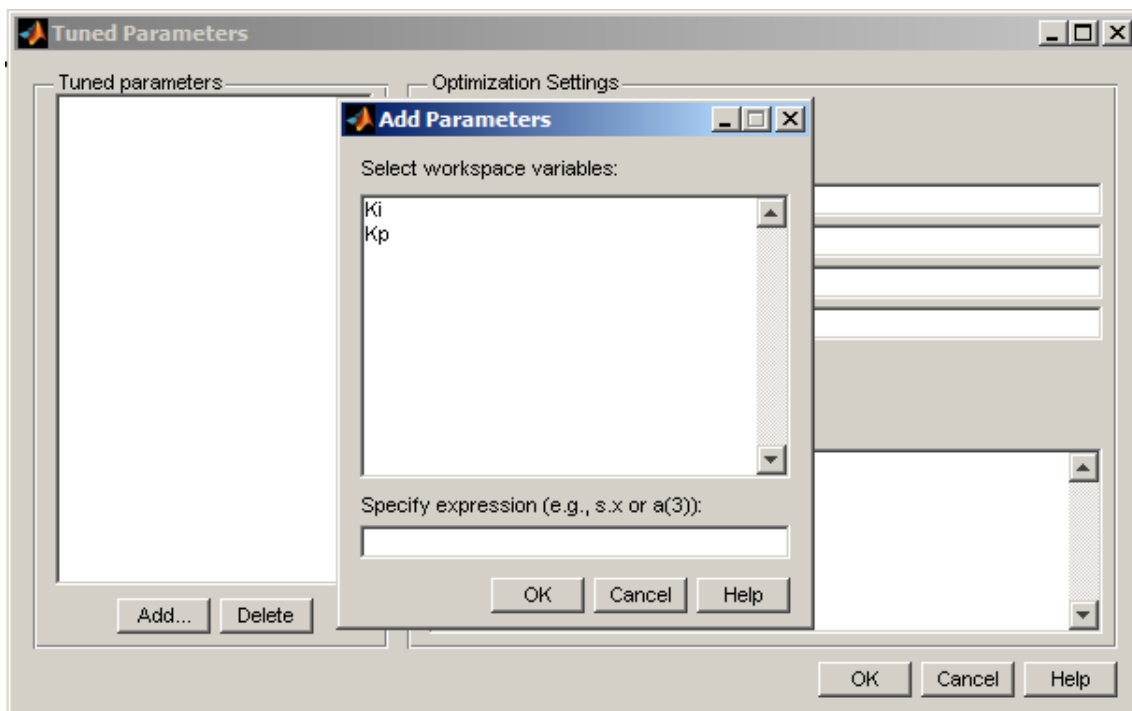


Figure 11. Introducing of PI parameters to Signal Constraint block as a variable

After all this, the optimization process is started. The result of the optimization process may take a period of 3-4 hours, depending on the state of the limit values. In this optimization, if the limit values are too suppressed, the operation will fail (Figure 12). If the limit values are re-entered with a little more tolerance, it will be possible to achieve the desired result in the optimization process.

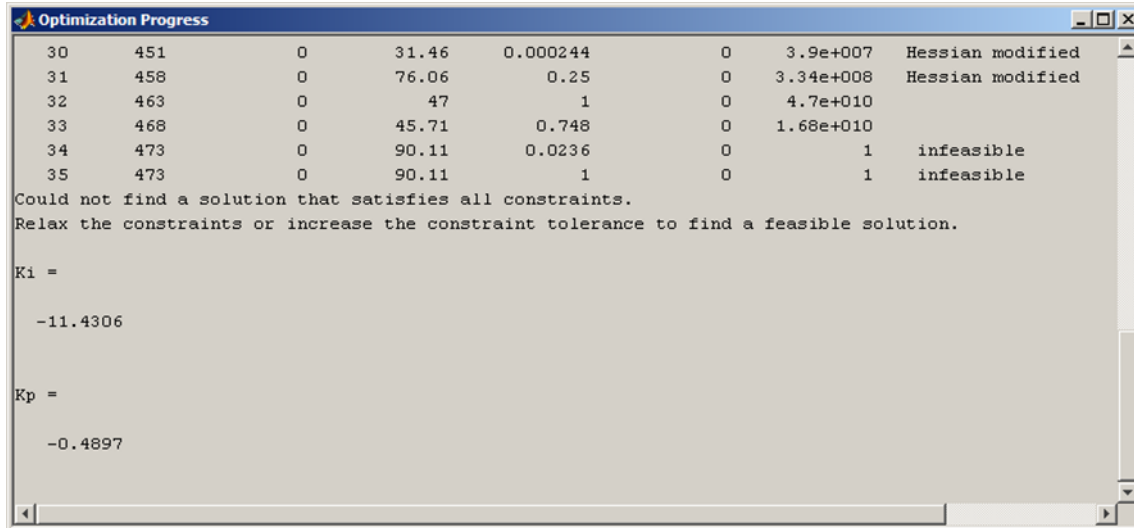


Figure 12. Screenshot showing optimization failed

After the optimization process, the values of K_p=0,1786 and K_i = 1,87 were reached.

6. INTERFACES USED DURING SIMULATION

The motor parameters used in the simulation were collected at a point. This made easier to enter the data and to repeat for different values. The motor temperature was also included in the calculation to see the effect of the change in winding temperature on winding resistance and thus on current and other data and to make the simulation more realistic. In the catalog information of PMSM used in the experimental study, the values of winding resistances for 20 °C and 150 °C are given as 13.55 Ω and 18.25, respectively. In light of this information, the winding resistance corresponding to the temperature reached by the motor during the experiments was calculated by Eq. (8).

$$R_2 = R_1 [1 + \alpha_1(t_2 - t_1)] \quad (8)$$

In the equation, R_1 represents the winding resistance at t_1 temperature, R_2 is the winding resistance at t_2 temperature. α_1 is the resistance temperature coefficient at t_1 temperature and was calculated as 0.002668.

The interface designed for entering the motor parameters is shown in Figure 13 (a). The values in the interface are those of the PMSM used in the experimental study. The interface of the field-oriented PWM driver used to drive the PMSM is given in Figure 13 (b). Via to this interface shown in Figure 13 (b), it is much easier to see the responses of the motor for different speed, switching frequency, PI values, and hysteresis band. Since the switching frequency of the driver was 8 kHz, the switching frequency was also taken as 8 kHz. All values except Kp and Ki in the interface are the actual values of the motor and driver.

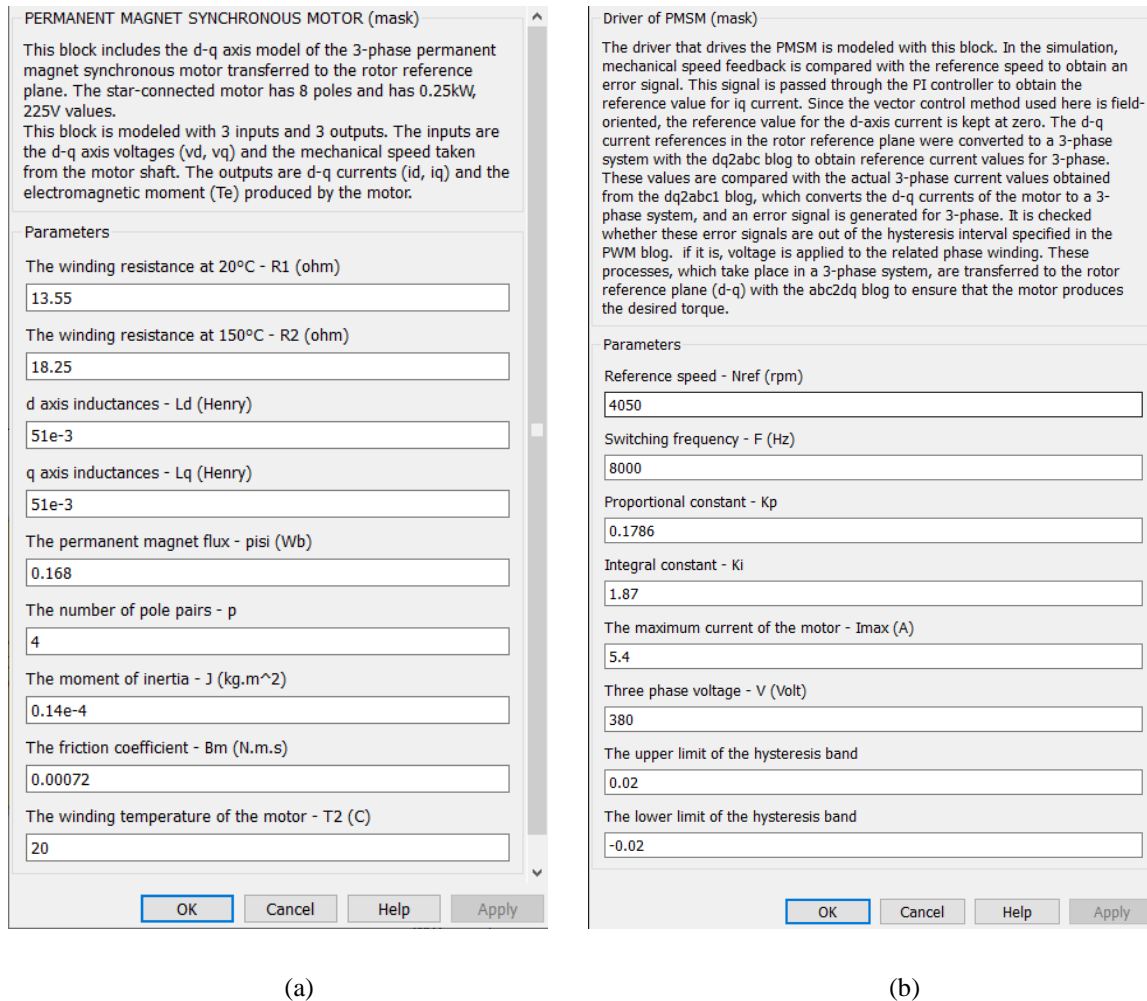


Figure 13. The interfaces designed for entering of parameters (a) For PMSM (b) For driver

The interface of the torque block that allows the motor to be loaded at different values is shown in Figure 14. Via to this interface, it is possible to change the value of the load applied to the motor shaft at any time and examine the response of the motor to different loads.

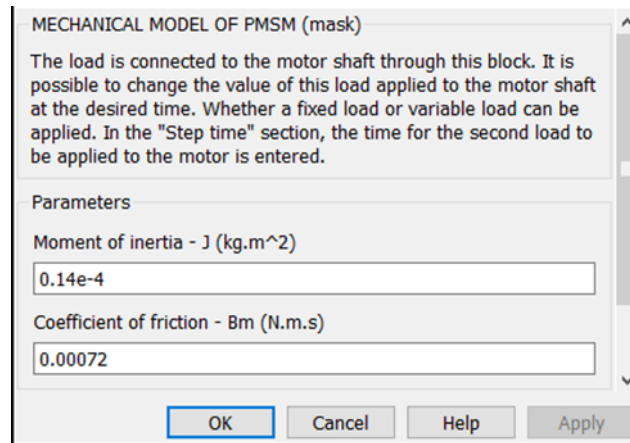


Figure 14. Interface of the torque block that allows the motor to be loaded with different loads

7. THE EXPERIMENT AND SIMULATION RESULTS

The label information of 8-pole PMSM used during experimental study is shown in Figure 15. Figure 16 shows the layout of the experimental work. As can be seen in Figure 16, DC Generator is coupled to the motor shaft in order to load the PMSM. The generator is manufactured by the company named KORMAS with product code 671 150 01 (12V) and has plate values of 12 V, 0.8A-13A, 190 W, 2900 rpm. The generator is loaded by using 12 V, 20 W lamps.

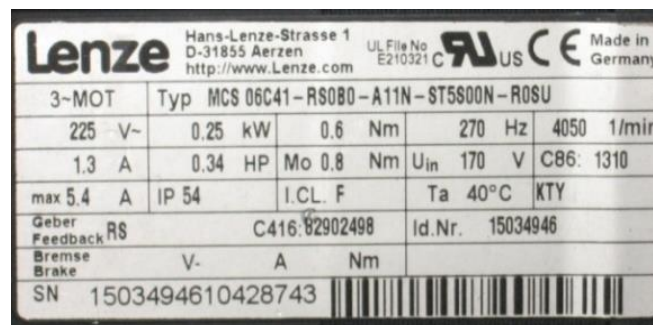


Figure 15. The PMSM label used during experiment

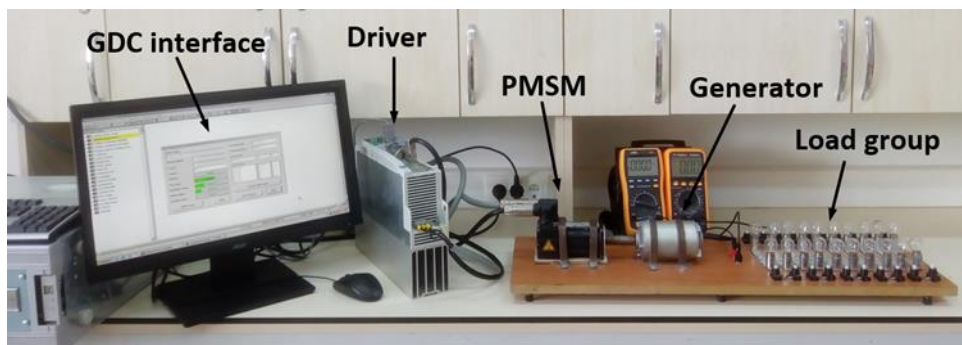


Figure 16. Experimental set-up

The driver which was manufactured by LENZE with EVS9322-ESV004 product code was used for driving the motor. The Global Drive Control (GDC) is an interface program which is produced by the company in order to provide programming of 8200 and 9300 driver series by users.

The speed, current, resistance and torque values of the motor and the temperatures of motor and cooler have been obtained by GDC and by other various measurement devices. The calculations show that when the generator is connected to the shaft of the PMSM without load, the generator causes an additional load of 16W. The calculation is as follows:

GDC interface program was used to calculate shaft power. The generator was coupled to PMSM in no-load condition and the motor operated at its rated speed. Torque and speed information was achieved from GDC. This information was included in the Eq. (9) and the shaft power of the motor was calculated as 38 W. Afterwards the generator which was coupled to the motor shaft was removed and the motor was re-operated. Torque and speed values were re-achieved from GDC. In this situation, the shaft power of the motor was calculated as 22 W. Finally, taking the difference of these two values, the load caused by the unloaded generator was calculated.

$$P_{shaft} = T \cdot \omega_r \quad (9)$$

The expressions P_{shaft} and T in Eq. (9) symbolize the shaft power and torque of the motor, respectively.

Firstly, PMSM was loaded with a full load. To achieve this, all the lamps connected to the generator were switched on. Then the same experiment was repeated by gradually reducing the number of lamps. In this case, the power provided to the lamps by the generator with an armature winding resistance of 0.3 Ω and the shaft power of PMSM is seen in detail in Table 1. Since the motor speed oscillates between 4020 and 4050 rpm in the experiments, the average value (4035 rpm) was given in Table 1.

The torque calculated as a result of the experiment, and the temperature of the motor reached during the experiment were entered into the interface, then the simulation was started. Since the experiments were performed at the nominal speed, the simulations were performed at the nominal speed. Speed, torque and current curves were obtained from the simulations performed for each load stage separately. The speed, current and torque values obtained from

the simulations where the reference speed is entered as 4050 rpm are presented in Table 1 together with the experiment results.

Experimental and simulation results were obtained for 10 different load stages. However, here, the curves of the torque, speed, and effective value of the phase currents obtained from the simulation for only full load (0.62 Nm) operation were given. These curves are seen in Figure 17.

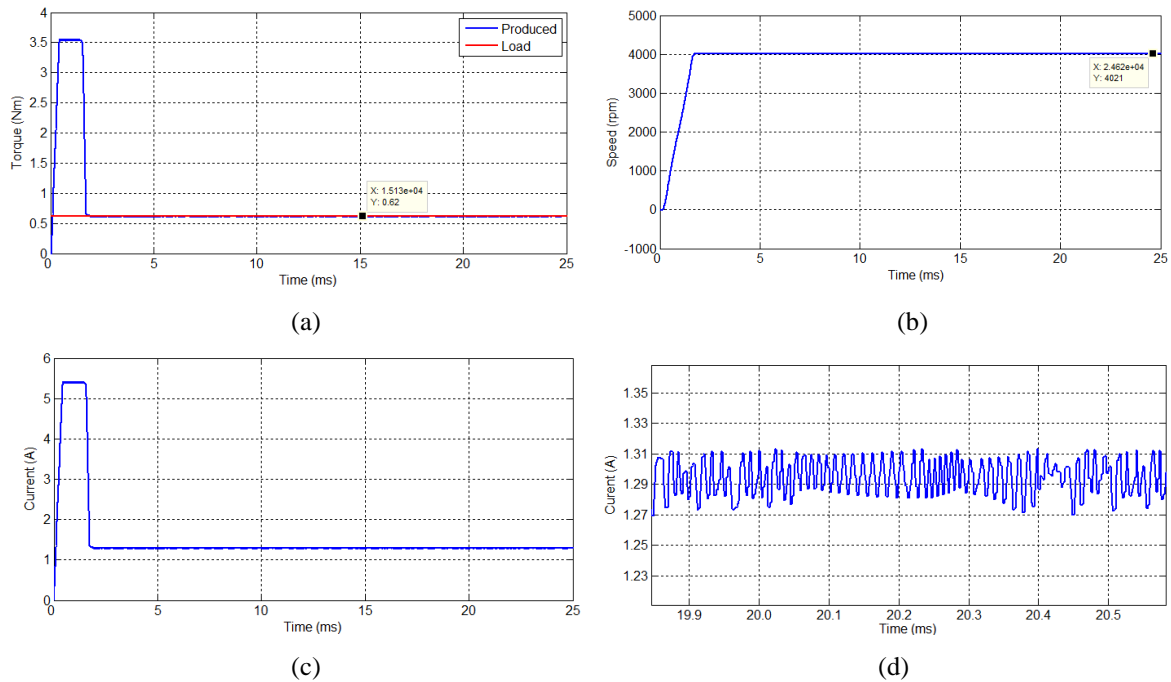


Figure 17. The simulation results for 0,62 Nm (a) Torque (b) Speed (c) The rms value of phase current (d) The enlarged version of the phase current rms value for a certain range

The experiment and simulation results of PMSM's rated speed are given in Table 1. When Table 1 is examined, it is seen that the experimental and simulation results are very close to each other in the regions where the motor is tried to load at rated power. If the results are evaluated separately for torque, current, and speed:

- The simulation produces the desired torque value accurately in accordance with the hysteresis band of the driver.
- The speed results obtained from the simulation are within the speed range between 4020 rpm and 4050 rpm. The only difference is the 10 rpm when the motor is no-load. This is a 0.2 % error and is negligible.
- When the current results are compared, it is seen that the results are very close to each other in the rated power of the motor and the regions close to it. For example, when the

simulation results of 0.62 Nm are examined, it is seen that the motor phase current is obtained as 1.30 A in the experiment and 1.29 A in the simulation. The difference of 0.01 is a 0.7 % error and it occurred because of the above-mentioned assumes. In regions close to the no-load operation, there is a difference of 0.13 A between the results. These differences are due to the measuring instrument.

Table 1. Experimental and simulation results at rated speed

Number of loads	PMSM's Measurement Results			Results of DC Generator					Calculation Results of PMSM		Simulation Results				Error	
				Measurement		Calculation										
	T (°C)	n (d/d)	I (A)	I (A)	U (V)	P (W)	P _{cu} (W)	∑P (W)	P _{shaft} (W)	T _e (Nm)	T _e (N.m.)	I (A)	n (d/d)	e _i (A)	e _m (Nm)	
20	41	4035	1,3	20,5	5,8	119	127	245	261	0,62	0,62	1,29	4021	0,01	0	
18	45	4035	1,25	19,1	6	115	109	224	240	0,57	0,57	1,22	4024	0,03	0	
16	49	4035	1,16	17,8	6,5	115	96	211	227	0,54	0,54	1,18	4026	-0,02	0	
14	51	4035	1,12	17,1	6,6	113	88	201	217	0,51	0,51	1,14	4028	-0,02	0	
12	52	4035	1,01	15	7,5	112	67	179	195	0,46	0,46	1,07	4031	-0,06	0	
10	54	4035	0,97	14,1	7,8	110	59	169	185	0,44	0,44	1,04	4033	-0,07	0	
8	54	4035	0,83	11,4	9,1	104	39	143	159	0,38	0,38	0,96	4037	-0,13	0	
6	54	4035	0,74	9,2	10,1	93	26	118	134	0,32	0,32	0,87	4041	-0,13	0	
4	54	4035	0,61	6,6	11,3	75	13	88,1	104	0,25	0,25	0,78	4046	-0,17	0	
0	45	4035	0,36	-	15,3	-	-	-	38	0,04	0,04	0,48	4060	-0,12	0	

8. TESTING OF SIMULINK MODEL AT DIFFERENT SPEED AND DIFFERENT LOAD LEVELS

Experiment and simulation results of PMSM with different speed and load levels are given in Table 2. The experiments are repeated at speeds 3000 rpm and 3500 rpm with different load levels. During the experiments where the reference speed was 3000 rpm, the speed of the motor varied from 2970 rpm to 3000 rpm. Therefore, the average of these values (2985 rpm) is given in the table. Similarly, in experiments where the reference speed was 3500 rpm, the speed of the motor varied from 3470 rpm to 3500 rpm. Therefore, 3485 rpm, which is the average of these values, was written in the table. So, no separate column was created for speed error in the table.

Table 2. Experimental and simulation results at different speed and load levels

Number of loads	PMSM's Measurement Results			Results of DC Generator					Calculation Results of PMSM		Simulation Results			Error	
				Measurement		Calculation									
	T (°C)	n (d/d)	I (A)	I (A)	U (V)	P (W)	P _{cu} (W)	ΣP (W)	P _{shaft} (W)	T _e (Nm)	T _e (N.m.)	I (A)	n (d/d)	e _i (A)	e _m (Nm)
19	44	3485	1,14	17,04	5,76	98,2	87,1	185,3	201,3	0,55	0,55	1,14	3471	0,00	0
12	49	3485	0,94	13,62	6,86	93,4	55,7	149,1	165,1	0,45	0,45	1,00	3476	0,06	0
4	35	3485	0,62	6,19	10,48	64,9	11,5	76,4	92,4	0,25	0,25	0,72	3490	0,10	0
19	48	2985	1,02	15,85	4,50	71,3	75,4	146,7	162,7	0,52	0,52	1,05	2967	0,03	0
12	50	2985	0,84	12,06	5,96	71,9	43,6	115,5	131,5	0,42	0,42	0,91	2974	0,07	0
4	38	2985	0,57	5,67	8,90	50,5	9,6	60,1	76,1	0,24	0,24	0,65	2987	0,08	0

If the results in Table 2 are evaluated separately for torque, current, and speed:

- The simulation produces the desired torque values accurately in accordance with the hysteresis band of the driver.
- The speed values obtained from the simulation are within the speed range obtained in the experiment.
- When the current values are compared, it is seen that the results are very close to each other in the rated power of the motor and the regions close to it.

9. TESTING OF SIMULINK MODEL ON A DIFFERENT PMSM

The Simulink model will be applied to another PMSM and the accuracy of the model will be tested in this section. The PMSM parameters that will be used in the simulation belongs to the experimental study in (Güngör et al., 2007). The parameters of the PMSM used in the corresponding experimental study have been shown in Table 3.

Table 3. The characteristics of PMSM to be used in testing the model

Company	Lenze	Rated voltage (V)	330
Pole number	6	Rated frequency (Hz)	190
Rated speed (rpm)	3800	Moment of inertia (kg m ² . 10 ⁻⁴)	1,2
Rated torque (Nm)	2,8	Resistance of stator coil (Ω)	5,2
Rated power (kW)	1,1	d-q axis inductances (mH)	16
Rated current (A)	2,3	Flux linkages of rotor (Wb)	0,345

Reference: Güngör et al., 2007

The simulation was started after the motor parameters in Table 3 were entered into the interfaces created in the model. In the study in (Güngör et al., 2007), no-load operation and 1

Nm load tests were performed. Then the speed, torque and iq current curves of the motor were given. However, the current value of the motor, which is one of the important data during the experimental study, is not known. For this reason, during the simulation, the motor was loaded with a load of 2.8 Nm, which is the rated torque, and the state of the rated speed and rated current on the motor label was examined. The simulation results obtained for the effective value of torque, speed and phase currents are seen in Figure 18.

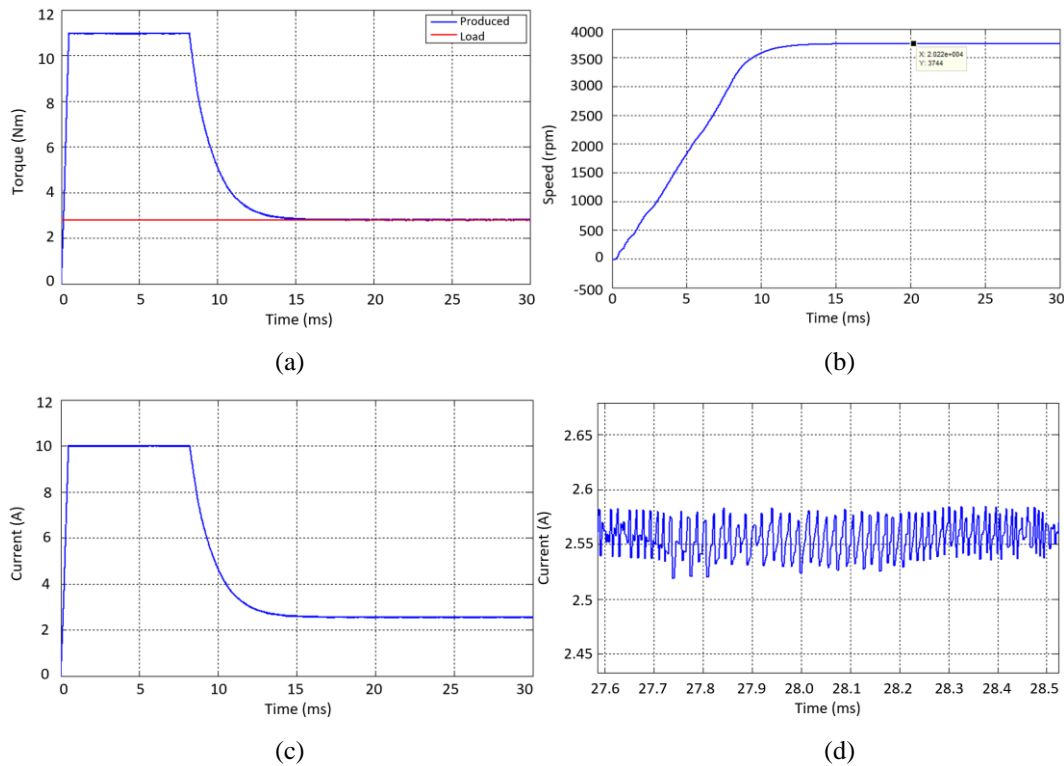


Figure 18. The simulation results for 2,8 Nm (a)Torque (b) Speed (c) The rms value of phase current (d) The enlarged version of the phase current rms value for a certain range

When the simulation results in Figure 18 are examined, it is seen that the motor accurately compensates the load torque in accordance with the hysteresis band which is determined by the driver.

- The motor accurately compensates the load torque in accordance with the hysteresis band which is determined by the driver.
- The motor accelerates stably at 15 ms without any oscillation and reaches 3744 rpm. Although the rated speed is 3800 rpm on label information, how much speed rpm does the motor speed reaches is not known during operation. Therefore the motor has produced an error of 56 rpm according to label information. And this corresponds to 1.47 % speed error.

- The motor draws a current of 2.55 A at full load. Therefore, there is a current error of 0.25 A according to the label information. However, since there is no experimental study on the full load condition of the related motor, it will not be healthy to make an exact error estimate for the motor speed and the current in full load condition.

10. CONCLUSIONS

In this study, PMSM was simulated based on the FOC method. It was seen that the current results obtained from experimental studies and simulations for 0.25 kW PMSM coincide with a negligible error percentage in the regions close to the rated power of the motor. In the simulation, where the driver produced the desired moment within the limits of the designed hysteresis band, the speed response was also within the limits measured in the experiment and it was seen that there is an acceptable speed error of 0.2 % only when the motor is no-load.

In order to test the validity of simulation, simulation results were compared according to label information of another PMSM (1.1 kW). During the comparison, it was seen that the motor produced the load torque accurately according to the desired hysteresis band and reached to rated speed entered as a reference with an error of 1.47 %. The current, 0.25 A exceeded.

In this study, it was tried to reach the goal of contributing to design and development studies by examining the current, velocity and moment responses of different PMSMs to different loads without performing experimental studies. This study is of particular importance in terms of optimizing PI controller parameters with the Signal Constraint Block in the Simulink Response Optimization toolbox, including winding temperature in the simulation, and plotting of the rms value curves of the current.

ACKNOWLEDGE

This study was produced from Fatih Alpaslan KAZAN's master thesis named "Control of Permanent Magnet Synchronous Motor".

REFERENCES / KAYNAKLAR

Bilgin, O. & Kazan, F. A. (2016). The effect of magnet temperature on speed, current and torque in PMSMs. *Paper presented at the 2016 XXII International Conference on Electrical Machines (ICEM)*.

Chin, Y. & Soulard, J. (2003). A permanent magnet synchronous motor for traction applications of electric vehicles. *Paper presented at the IEEE International Electric Machines and Drives Conference, 2003 IEMDC'03*.

- Cui, B., Han, Z., Li, J. & Mu, J. (2019, 13-15 June). Research on PMSM speed control system based on improved reaching law. *Paper presented at the 3rd International Conference on Circuits, System and Simulation (ICCSS)*, Nanjing, China.
- Güngör, B., Özgenel, M. C. & Demirbaş, Ş. (2007). Performance analysis of vector controlled permanent magnet synchronous motor with space vector pulse width modulation. *Journal of Polytechnic*, 10(1), 7-13.
- Itoh, J.-I., Nomura, N. & Ohsawa, H. (2002). A comparison between V/f control and position-sensorless vector control for the permanent magnet synchronous motor. *Paper presented at the Proceedings of the Power Conversion Conference-Osaka 2002*.
- Juming, S., Ming, Z. & Yanmin, S. (2003). Study of optimal efficient control of permanent magnet synchronous motor. *Paper presented at the Sixth International Conference on Electrical Machines and Systems, 2003 ICEMS*.
- Kazan, F. A. (2009). *Control of permanent magnet synchronous motor* (Master's thesis). Selcuk University, Konya.
- Krause, P. C., Wasynczuk, O. & Sudhoff, S. D. (1986). *Analysis of electric machinery* (Vol. 564). New York: McGraw-Hill.
- Lu, Y., Xie, W., Qu, L. & Zhang, Y. (2011). Dynamic simulation of permanent magnet synchronous motor fed by voltage source inverter. *Paper presented at the 2011 International Conference of Information Technology, Computer Engineering and Management Sciences*.
- Modran, L. (2008). Digital simulation of induction and permanent magnet synchronous motor starting. *Paper presented at the 2008 11th International Conference on Optimization of Electrical and Electronic Equipment*.
- Muni, B., Pillai, S. & Saxena, S. (1996). Digital simulation of internal power factor angle controlled surface mounted permanent magnet synchronous motor. *Paper presented at the Proceedings of International Conference on Power Electronics, Drives and Energy Systems for Industrial Growth*.
- Pillay, P. & Krishnan, R. (1988). Modeling of permanent magnet motor drives. *IEEE Transactions on Industrial Electronics*, 35(4), 537-541.
- Pillay, P. & Krishnan, R. (1989). Modeling, simulation, and analysis of permanent-magnet motor drives. I. The permanent-magnet synchronous motor drive. *IEEE Transactions on Industry Applications*, 25(2), 265-273.
- Pillay, P. & Krishnan, R. (1991). Application characteristics of permanent magnet synchronous and brushless DC motors for servo drives. *IEEE Transactions on Industry Applications*, 27(5), 986-996.
- Ping, L. & Lan, C. (2012). Study on controlling and simulation of drive system for permanent magnet synchronous motor in electrical vehicle. *Paper presented at the 2012 Power Engineering and Automation Conference*.
- Song, L. & Peng, J. (2009). The study of fuzzy-PI controller of permanent magnet synchronous motor. *Paper presented at the 2009 IEEE 6th International Power Electronics and Motion Control Conference*.
- Xia, Y., Yi, X., Wen, Z., Chen, Y. & Zhang, J. (2019). Direct torque control of hybrid excitation permanent magnet synchronous motor. *Paper presented at the 2019 22nd International Conference on Electrical Machines and Systems (ICEMS)*.
- Xiao-Ling, Y. & Hong-Hua, W. (2009). Intelligent sensorless control of permanent magnet synchronous motor drive. *Paper presented at the 2009 Second International Conference on Intelligent Computation Technology and Automation*.